Pis'ma v ZhETF, vol. 94, iss. 5, pp. 387 – 392

Nonplanar double layers in plasmas with opposite polarity dust

A. A. Mamun[1)2)], *A. Mannan*

Department of Physics, Jahangirnagar University, Savar, Dhaka-1342, Bangladesh

Submitted 20 June 2011
Resubmitted 11 July 2011

Nonplanar (cylindrical and spherical) double layers (DLs) in a four-component dusty plasma (composed of inertial positively and negatively charged dust, Boltzmann electrons and ions) are studied by employing the reductive perturbation method. The modified Gardner (mG) equation describing the nonlinear propagation of the dust-acoustic (DA) waves is derived, and its nonplanar double layer solutions are numerically analyzed. The parametric regimes for the existence of the DLs, which are found to be associated with positive potential only, are obtained. The basic features of nonplanar DA DLs, which are found to be different from planar ones, are also identified. The implications of our results to different space and laboratory dusty plasma situations, where opposite polarity dust are observed, are discussed.

I. Introduction. There has been a great deal of interest in understanding linear and nonlinear features of the novel dust acoustic (DA) waves [1], not only because they exist in both space and laboratory dusty plasmas [2, 3], but also because they triggered a number of remarkable laboratory experiments [4–8]. Rao et al. [1] have first theoretically predicted the existence of this novel extremely low phase velocity (in comparison with the electron and ion thermal velocities) DA-waves, where the dust mass provides the inertia and the electron and ion thermal pressures give rise to the restoring force. The prediction of Rao et al. [1] has then conclusively verified by a number of laboratory experiments [4–6]. The linear features of the novel DA-waves have also been extensively studied for some other situations [9–11].

Rao et al., in their seminal work [1], have also studied small, but finite amplitude DA solitary waves. Mamun et al. [12] and Mamun [13] have then generalized the work of Rao et al. [1] to study arbitrary amplitude solitary waves. The nonlinear DA-waves have also been rigorously investigated by many authors for different dusty plasma situations theoretically [14–28] as well as experimentally [7, 8] during last two decades. However, all of these works on nonlinear DA-waves [1, 12–28] are based on the most commonly used dusty plasma model that assumes negatively charged dust. The consideration of negatively charged dust is due to the fact that in low-temperature laboratory plasmas, collection of plasma particles (viz. electrons and ions) is the only important charging process, and the thermal speeds of electrons far exceeds that of ions. But, there are some other more important charging processes by which dust grains become positively charged [29–32]. The principal mechanisms by which dust grains become positively charged are photoemission in the presence of a flux of ultraviolet photons [29, 30], thermionic emission induced by radiative heating [31], secondary emission of electrons from the surface of the dust grains [32], etc.

There is direct evidence of the coexistence of positively and negatively charged dust in different regions of space, viz. Earth's mesosphere [33], cometary tails [34, 35], Jupiter's magnetosphere [35, 36], etc. Chow et al. [32] have theoretically shown that due to the size effect on secondary emission, insulating dust grains with different sizes can have the opposite polarity, smaller ones being positive and larger ones being negative. The opposite situation, i.e. larger (massive) ones being positive and smaller (lighter) ones being negative, is also possible by triboelectric charging [37, 38]. This is predicted from the observations of dipolar electric fields perpendicular to the ground, with negative pole at higher altitudes, generated by dust devils [39, 40] and sand storms [41]. The formation of these dipolar electric fields means that negatively charged smaller (i.e. lighter) dust are blown upward in the convection, while positively charged larger (more massive) dust remain the surface due to gravity. It is shown by experiments using Mars dust analogous in Mars simulation wind tunnel that μ-sized dust can carry net charges of around $10^5 e$, and there could be almost equal quantities of positively and negatively charged dust in the suspension [37, 40].

The coexistence of positively and negatively charged dust, with larger (massive) dust being positive and smaller (lighter) dust being negative [42–44] or vice versa [45], is also observed in laboratory devices [42–45] where dust of polymer materials are used. It may be noted

[1)] Present adress: The Abdus Salam International Centre for Theoretical Physics, 34014 Trieste, Italy
[2)] e-mail: mamun_phys@yahoo.co.uk

here that the coexistence of same sized dust of opposite polarity may also occur by photoemission if the photoemission yields of the dust-material are very different [46].

Recently, motivated by these theoretical predictions and satellite/experimental observations, a number of authors [37, 47–52] have considered a dusty plasma with dust of opposite polarity, and have investigated linear [48, 37] and nonlinear [47, 49–52] DA-waves. However, all of these studies are limited to one-dimensional planar geometry, which may not be the realistic situation in space and laboratory devices, since the waves observed in space (laboratory devices) are certainly not infinite (unbounded) in one-dimension (1D). The most of these works on nonlinear DA-waves are also concerned with either solitary or shock structures, but not with double layers. Therefore, in our present work, we consider a dusty plasma system (consisting of positively and negatively charged dust fluid, Boltzmann electrons and ions) and a more general geometry (which is valid for both planar, cylindrical and spherical geometries), and theoretically study the basic features of the DA DLs that are found to exist in such a realistic novel dusty plasma system.

The paper is organized as follows. The basic equations governing the dynamics of the DA-waves is presented in section II. The modified Gardner (mG) equation is derived in section III. The numerical analysis of mG-equation along with a brief discussion is presented in section IV.

II. Governing Equations. We consider the nonlinear propagation of the DA-waves in an unmagnetized nonplanar dusty plasma system containing positively and negatively charged dust fluid, Boltzmann electrons and ions. Thus, at equilibrium, we have $n_{i0} + Z_p n_{p0} = n_{e0} + Z_n n_{n0}$, where n_{i0}, n_{p0}, n_{e0}, n_{n0} are, respectively ion, positive dust, electron, and negative dust number density at equilibrium, and Z_p (Z_n) represents the charge state of positive (negative) dust. The nonlinear dynamics of the DA-waves propagating in such a nonplanar dusty plasma is governed by

$$\frac{\partial n_n}{\partial t} + \frac{1}{r^\nu}\frac{\partial}{\partial r}(r^\nu n_n u_n) = 0, \tag{1}$$

$$\frac{\partial u_n}{\partial t} + u_n\frac{\partial u_n}{\partial r} = \frac{\partial \phi}{\partial r}, \tag{2}$$

$$\frac{\partial n_p}{\partial t} + \frac{1}{r^\nu}\frac{\partial}{\partial r}(r^\nu n_p u_p) = 0, \tag{3}$$

$$\frac{\partial u_p}{\partial t} + u_p\frac{\partial u_p}{\partial r} = -\alpha\frac{\partial \phi}{\partial r}, \tag{4}$$

$$\frac{1}{r^\nu}\frac{\partial}{\partial r}\left(r^\nu\frac{\partial \phi}{\partial r}\right) = -\rho, \tag{5}$$

$$\rho = \mu_i e^{-\phi} - \mu_e e^{\sigma\phi} + \mu_p n_p - n_n, \tag{6}$$

where $\nu = 0$ for $1D$ planar geometry, and $\nu = 1$ (2) for a nonplanar cylindrical (spherical) geometry; n_p (n_n) is the positive (negative) dust number density normalized by its equilibrium value n_{p0} (n_{n0}); u_p (u_n) is the positive (negative) dust fluid speed normalized by $C_d = (Z_n k_B T_i/m_n)^{1/2}$; ϕ is the electrostatic wave potential normalized by $k_B T_i/e$; ρ is the surface charge density normalized by $Z_n e n_{n0}$; $\sigma = T_i/T_e$, $\alpha = Z_p m_n/Z_n m_p$, $\mu_e = n_{e0}/Z_n n_{n0}$, $\mu_i = n_{i0}/Z_n n_{n0}$, $\mu_p = Z_p n_{p0}/Z_n n_{n0} = 1+\mu_e-\mu_i$, m_n (m_p) is the mass of the negative (positive) dust, T_i (T_e) is the ion (electron) temperature, k_B is the Boltzmann constant, and e is the magnitude of the electron-charge. The time and space variables are in units of the negative dust plasma period $\omega_{pn}^{-1} = (m_n/4\pi e^2 Z_n^2 n_{n0})^{1/2}$, and the Debye-radius $\lambda_{Dm} = (Z_n k_B T_i/4\pi e^2 Z_n^2 n_{n0})^{1/2}$, respectively.

III. Derivation of mG-Equation. To study finite amplitude DA DLs by the reductive perturbation method [53, 54], we first introduce the stretched coordinates:

$$\zeta = \epsilon(r - V_p t), \tag{7}$$

$$\tau = \epsilon^3 t, \tag{8}$$

where ϵ is a small parameter ($0 < \epsilon < 1$) measuring the weakness of the dispersion, and V_p (normalized by C_d) is the phase speed of the perturbation mode, and expand all the dependent variables (viz. n_n, n_p, u_n, u_p, ϕ, and ρ) in power series of ϵ:

$$n_n = 1 + \epsilon n_n^{(1)} + \epsilon^2 n_n^{(2)} + \epsilon^3 n_n^{(3)} + \cdots, \tag{9}$$

$$n_p = 1 + \epsilon n_p^{(1)} + \epsilon^2 n_p^{(2)} + \epsilon^3 n_p^{(3)} + \cdots, \tag{10}$$

$$u_n = 0 + \epsilon u_n^{(1)} + \epsilon^2 u_n^{(2)} + \epsilon^3 u_n^{(3)} + \cdots, \tag{11}$$

$$u_p = 0 + \epsilon u_p^{(1)} + \epsilon^2 u_p^{(2)} + \epsilon^3 u_p^{(3)} + \cdots, \tag{12}$$

$$\phi = 0 + \epsilon \phi^{(1)} + \epsilon^2 \phi^{(2)} + \epsilon^3 \phi^{(3)} + \cdots, \tag{13}$$

$$\rho = 0 + \epsilon \rho^{(1)} + \epsilon^2 \rho^{(2)} + \epsilon^3 \rho^{(3)} + \cdots. \tag{14}$$

Now, expressing (1)–(6) in terms of ζ and τ, and substituting (9)–(14) into the resulting equations ((1)–(6) expressed in terms of ζ and τ), one can easily develop different sets of equations in various powers of ϵ. To the lowest order in ϵ one obtains

$$u_p^{(1)} = \frac{\alpha\psi}{V_p}, \quad n_p^{(1)} = \frac{\alpha\psi}{V_p^2}, \quad u_n^{(1)} = -\frac{\psi}{V_p}, \tag{15}$$

$$n_n^{(1)} = -\frac{\psi}{V_p^2}, \quad \rho^{(1)} = 0, \quad V_p^2 = \frac{1+\alpha\mu_p}{\mu_i + \mu_e\sigma}, \tag{16}$$

where $\psi = \phi^{(1)}$. The expression for V_p^2 in (16) represents the linear dispersion relation for the DA-waves

propagating in a dusty plasma under consideration. To the next higher order in ϵ, we obtain another set of equations, which, after using (15), (16), can be simplified as

$$u_p^{(2)} = \frac{\alpha^2\psi^2}{2V_p^3} + \frac{\alpha\phi^{(2)}}{V_p},\ n_p^{(2)} = \frac{3\alpha^2\psi^2}{2V_p^4} + \frac{\alpha\phi^{(2)}}{V_p^2}, \tag{17}$$

$$u_n^{(2)} = \frac{\psi^2}{2V_p^3} - \frac{\phi^{(2)}}{V_p},\ n_n^{(2)} = \frac{3\psi^2}{2V_p^4} - \frac{\phi^{(2)}}{V_p^2}, \tag{18}$$

$$\rho^{(2)} = \frac{1}{2}A\psi^2 = 0,\ A = \mu_i - \mu_e\sigma^2 - \frac{3}{V_p^4}(1-\mu_p\alpha^2). \tag{19}$$

It is obvious from (19) that $A = 0$ since $\phi^{(1)} \neq 0$. The solution of $A = 0$ for α is given by

$$\alpha = \alpha_c = \frac{1}{2C_1}[-C_2 \pm \sqrt{C_2^2 - 4C_1C_3}], \tag{20}$$

where

$$C_1 = \mu_p\mu_i(\mu_p + 3\mu_i + 6\mu_e\sigma) + \mu_e\mu_p\sigma^2(3\mu_e - \mu_p),$$
$$C_2 = 2\mu_p(\mu_i - \mu_e\sigma^2),$$
$$C_3 = \mu_i(1 - 3\mu_i - 6\mu_e\sigma) - \mu_e\sigma^2(1 + 3\mu_e).$$

It is obvious that (19) is satisfied for $\alpha = \alpha_c$. We have numerically shown how α_c varies with μ_e and μ_i for a fixed $\sigma = 0.1$. The results are displayed in Fig. 1 which

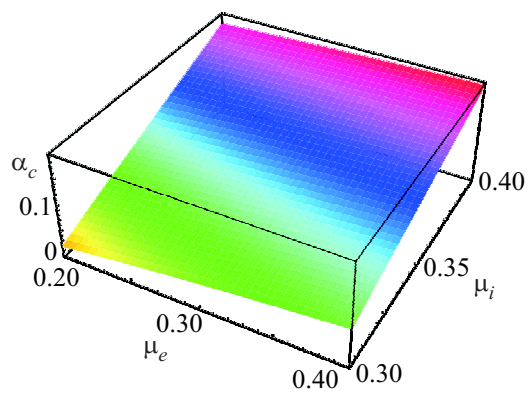

Fig. 1. (Color online) Showing how α_c (obtained from $A(\alpha = \alpha_c) = 0$) varies with μ_e and μ_i for $\sigma = 0.1$

in fact represents the $A = 0$ surface plot, and provides us the parametric regimes (which correspond to above or below the $A = 0$ surface plot) of our present interest. So, for α around its critical value (α_c), i.e. for $|\alpha - \alpha_c| = \epsilon$ corresponding to $A = A_0$, we can express A_0 as

$$A_0 \simeq s\left(\frac{\partial A}{\partial \alpha}\right)_{\alpha=\alpha_c} |\alpha - \alpha_c| = sA_\mu\epsilon, \tag{21}$$

where $A_\mu = 6\mu_p(\mu_i + \mu_e\sigma)^2(1+\alpha_c)/(1+\mu_p\alpha_c)^3$, and $s = 1$ for $\alpha > \alpha_c$ and $s = -1$ for $\alpha < \alpha_c$. So, for $\alpha \neq \alpha_c$, we can express $\rho^{(2)}$ as

$$\rho^{(2)} \simeq \frac{1}{2}s\epsilon A_\mu\psi^2. \tag{22}$$

This means that for $\alpha \neq \alpha_c$, $\rho^{(2)}$ must be included in the third order Poisson's equation. To the next higher order in ϵ, we obtain the third set of equations:

$$\frac{\partial n_n^{(1)}}{\partial\tau} + \frac{\nu u_n^{(1)}}{V_p\tau} - V_p\frac{\partial n_n^{(3)}}{\partial\zeta} + \frac{\partial F_n}{\partial\zeta} = 0, \tag{23}$$

$$\frac{\partial n_p^{(1)}}{\partial\tau} + \frac{\nu u_p^{(1)}}{V_p\tau} - V_p\frac{\partial n_p^{(3)}}{\partial\zeta} + \frac{\partial F_p}{\partial\zeta} = 0, \tag{24}$$

$$\frac{\partial u_n^{(1)}}{\partial\tau} - V_p\frac{\partial u_n^{(3)}}{\partial\zeta} + \frac{\partial}{\partial\zeta}\left[u_n^{(1)}u_n^{(2)}\right] - \frac{\partial\phi^{(3)}}{\partial\zeta} = 0, \tag{25}$$

$$\frac{\partial u_p^{(1)}}{\partial\tau} - V_p\frac{\partial u_p^{(3)}}{\partial\zeta} + \frac{\partial}{\partial\zeta}\left[u_p^{(1)}u_p^{(2)}\right] + \alpha\frac{\partial\phi^{(3)}}{\partial\zeta} = 0, \tag{26}$$

$$\frac{\partial^2\psi}{\partial\zeta^2} + \frac{1}{2}sA_\mu\psi^2 - (\mu_i + \mu_e\sigma)\phi^{(3)} + (\mu_i - \mu_e\sigma^2)\psi\phi^{(2)} - \frac{1}{6}(\mu_i + \mu_e\sigma^3)\psi^3 + \mu_p n_p^{(3)} - n_n^{(3)} = 0, \tag{27}$$

where $F_n = n_n^{(1)}u_n^{(2)} + n_n^{(2)}u_n^{(1)} + u_n^{(3)}$ and $F_p = n_p^{(1)}u_p^{(2)} + n_p^{(2)}u_p^{(1)} + u_p^{(3)}$. Now, using (15)–(19) and (23)–(27), we finally obtain a nonlinear dynamical equation of the form:

$$\frac{\partial\psi}{\partial\tau} + \frac{\nu}{2\tau}\psi + p\psi\frac{\partial\psi}{\partial\zeta} + q\psi^2\frac{\partial\psi}{\partial\zeta} + p_0\frac{\partial^3\psi}{\partial\zeta^3} = 0, \tag{28}$$

where $p = sA_\mu p_0$, $q = p_0 q_0$, and

$$p_0 = \frac{V_p^3}{2(1+\alpha\mu_p)}, \tag{29}$$

$$q_0 = \frac{15}{2V_p^6}(1 + \mu_p\alpha^3) - \frac{1}{2}(\mu_i + \mu_e\sigma^3). \tag{30}$$

Equation (28) is a modified Gardner (mG) equation. The modification is due to the extra term, $\frac{\nu}{2\tau}\psi$), which arises due to the effects of the nonplanar geometry. We have already mentioned that $\nu = 0$ corresponds to a $1D$ planar geometry which reduces (28) to a standard Gardner (sG) equation. Our aim now is to numerically analyze mG-equation. However, for clear understanding, we first briefly discuss the stationary DL-solution of this standard Gardner equation [i.e. (28) with $\nu = 0$].

The stationary DL-solution of the sG-equation (i.e. (28) with $\nu = 0$) is obtained by considering a moving frame (moving with speed U_0) $\xi = \zeta - U_0\tau$, and imposing all the appropriate boundary conditions for DL-solution, including $\psi \to 0$, $d\psi/d\xi \to 0$, $d^2\psi/d\xi^2 \to 0$ at $\xi \to -\infty$. These boundary conditions for the stationary DL-solution allow us to express the sG-equation (i.e. (28) with $\nu = 0$) as

$$\frac{1}{2}\left(\frac{d\psi}{d\xi}\right)^2 + V(\psi) = 0, \tag{31}$$

where the pseudo-potential $V(\psi)$ is

$$V(\psi) = -\frac{U_0}{2p_0}\psi^2 + \frac{sA_\mu}{6}\psi^3 + \frac{q_0}{12}\psi^4. \tag{32}$$

It is obvious from (32) that

$$V(\psi)\,|_{\psi=0} = \left.\frac{dV(\psi)}{d\psi}\right|_{\psi=0} = 0, \tag{33}$$

$$\left.\frac{d^2V(\psi)}{d\psi^2}\right|_{\psi=0} < 0. \tag{34}$$

The conditions (33) and (34), which are automatically satisfied, imply that the DL-solution of (31) exists if and only if

$$V(\psi)\,|_{\psi=\psi_m} = \left.\frac{dV(\psi)}{d\psi}\right|_{\psi=\psi_m} = 0, \tag{35}$$

where ψ_m is the amplitude of the DLs. The condition (35) can be expressed as

$$U_0 = -\frac{s^2A_\mu^2p_0}{6q_0}, \tag{36}$$

$$\psi_m = s\frac{6U_0}{A_\mu p_0}. \tag{37}$$

Now, using (32) and (37) in (31) we have

$$\frac{d\psi}{\psi(\psi_m - \psi)} = \sqrt{-\gamma}d\xi, \tag{38}$$

where $\gamma = q_0/6$. Now, integrating (38) the stationary DL-solution of sG-equation (i.e. (28) with $\nu = 0$) can be written as

$$\psi = \frac{\psi_m}{2}\left(1 + \tanh\frac{\xi}{\Delta}\right), \tag{39}$$

where Δ is the width of the DLs, and is given by

$$\Delta = \sqrt{\frac{24}{-\psi_m^2 q_0}}. \tag{40}$$

It is clear from (39) and (40) that DLs exist if and only if $q_0 < 0$, i.e. $\alpha_L < \alpha < \alpha_U$, where α_L (α_U), obtained from $q_0 = 0$, is the lower (upper) limit of α above (below) which DLs exist. We have graphically shown how α_U (upper surface plots of Figs. 2 and 3) and α_L (lower surface plots of Figs. 2 and 3) vary with μ_e, μ_i, and σ. On the other hand, since $p_0 > 0$ and $U_0 > 0$, (39) and (37) indicate that the DLs are associated with positive potential if $s = 1$, i.e. $\alpha > \alpha_c$, and associated with negative potential if $s = -1$, i.e. $\alpha < \alpha_c$. It is obvious

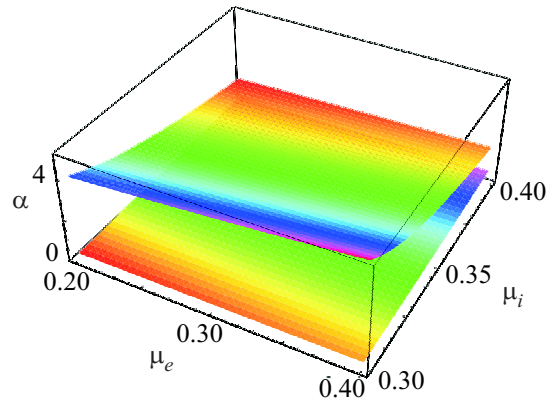

Fig. 2. (Color online) Showing the parametric regime for the existence of DLs (obtained from the solutions of $q_0 = 0$ for α) for $\sigma = 0.1$

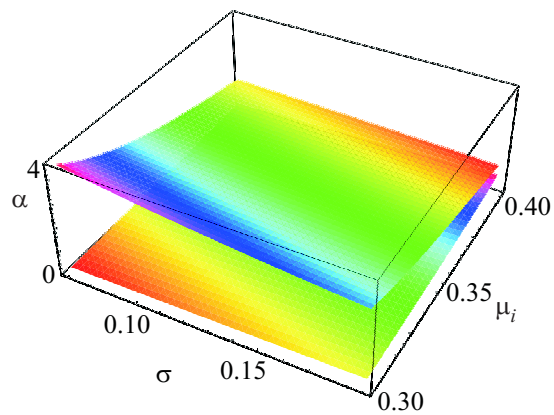

Fig. 3. (Color online) Showing the parametric regime for the existence of DLs (obtained from the solutions of $q_0 = 0$ for α) for $\mu_e = 0.2$

from Figs. 2 and 3 that $\alpha_L > \alpha_c$ which confirm us that DLs are associated with positive potential only. The parametric regimes for the existence of positive DLs are bounded by the lower and upper surface plot of Figs. 2 and 3, and DLs exist for parameters corresponding to any point in between two ($q_0 = 0$) surface plots.

It may be noted here that if we would neglect the higher order nonlinear term (viz. the fourth term of (28) or the term containing ψ^3), but would keep the lower order nonlinear term (viz. the third term of (28) or the term containing ψ^2), we would obtain the solitary structures that are due to the balance between nonlinearity (associated with ψ^2 only) and dispersion [1, 12, 13]. On the other hand, in our present work, we have kept both the terms containing ψ^2 and ψ^3, and have obtained the DL-structures which are formed due to the balance between the nonlinearity (associated with ψ^2 and ψ^3) and dispersion. It may be added here that the dissipation (which is usually responsible for the formation of the

shock-like structures [55, 20, 25]) is not essential for the formation of solitary and DL-structures [3, 56, 19]. The stationary DL-solution of the sG-equation, and the conditions for the existence of DLs clearly imply that the DL-structures predicted in our present investigation is not due to the dissipation (which has been neglected in our present investigation), but is due to the coexistence of positively and negatively charged dust.

IV. Numerical Analysis and Discussion. We now turn to (28) with the term $(\nu/2\tau)\psi$, which is due to the effects of the non-planar (cylindrical or spherical) geometry. An exact analytic solution of (28) is not possible. Therefore, we have numerically solved (28), and have studied the effects of cylindrical and spherical geometries on time-dependent DA DLs. The results are depicted in Figs. 4 to 5. The initial condition, that

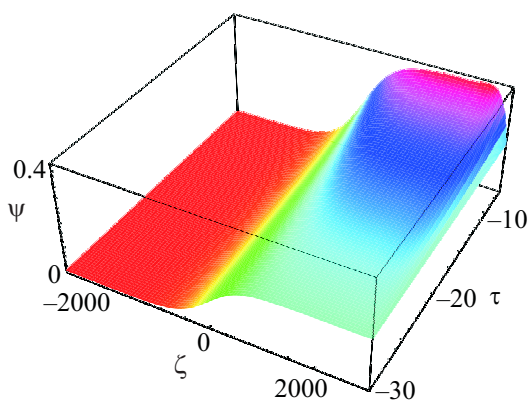

Fig. 4. (Color online) Showing the effects of cylindrical geometry on DA positive DLs for $\alpha = 0.615$, $\mu_e = 0.2$, $\mu_i = 0.4$, $\sigma = 0.1$, and $U_0 = 0.05$

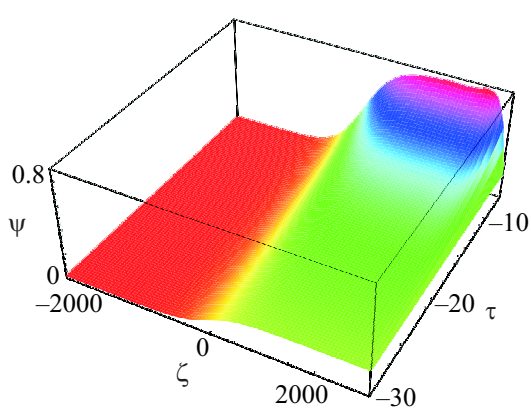

Fig. 5. (Color online) Showing the effects of spherical geometry on DA positive DLs for $\alpha = 0.615$, $\mu_e = 0.2$, $\mu_i = 0.4$, $\sigma = 0.1$, and $U_0 = 0.05$

we have used in our numerical analysis, is in the form of the stationary solution of (28) without the term $(\nu/2\tau)\psi$. Figures 4 (5) shows how the effects of cylindrical (spherical) geometry modify the DA DLs. The numerical solutions of (28) (displayed in Figs. 4 and 5) reveal that for a large value of τ (e.g. $\tau = -30$), the cylindrical ($\nu = 1$) and spherical ($\nu = 2$) DLs are almost similar to 1D planar ($\nu = 0$) structures. This is because for a large value of τ, the term $(\nu/2\tau)\psi$, which is due to the effects of the cylindrical or spherical geometry, is no longer dominant. However, as the value of τ decreases, the term $(\nu/2\tau)\psi$ becomes dominant, and spherical and cylindrical DL-structures differ from 1D planar ones. It is found that as the value of τ decreases, the amplitude of these localized pulses increases. It is also found that the amplitude of cylindrical DA-, DL-structures is larger than those of 1D planar ones, but smaller than that of the spherical ones. The amplitude of the DLs increases with the increase of U_0.

We have used a wide range of the dusty plasma parameters (viz. $\sigma = 0.07-0.19$, $\mu_e = 0.2-0.4$, and $\mu_i = 0.3-0.4$) in our numerical analysis. Thus, the dust-plasma parameters are within the appropriate ranges for both space environments [33–36, 39, 40], and laboratory devices [42–45]. The value of α for which the existence of the DLs is found, is also within the ranges of the dusty plasma parameters corresponding to dust-plasma parameters for both space environments [33–36, 39, 40], and laboratory devices [42–45]. To conclude, we hope that our results may be useful in understanding the localized electrostatic disturbances in both space environments [33–36, 39, 40], and laboratory devices [42–45].

The research grant for research equipment from the Third World Academy of Sciences, ICTP, Trieste, Italy is gratefully acknowledged. One of the authors (AAM) would like to thank Prof. Padma Shukla and Joseph Niemela for the useful discussions, Ms. Daniela Valentini for the administrative support, and the AS-ICTP for the financial support during his visit to the centre under the Associateship Scheme.

1. N. N. Rao, P. K. Shukla, and M. Y. Yu, Planet. Space Sci. **38**, 543 (1990).
2. F. Verheest, *Waves in Dusty Plasmas* (Kluwer Academic Publishers, Dordrecht, 2000).
3. P. K. Shukla and A. A. Mamun, *Introduction to Dusty Plasma Physics* (IoP Publishing Ltd., Bristol, 2002).
4. A. Barkan, R. L. Merlino, and N. D'Angelo, Phys. Plasmas **2**, 3563 (1995).
5. C. Thompson, A. Barkan, N. D'Angelo, and R. L. Merlino, Phys. Plasmas **4**, 2331 (1997).
6. R. L. Merlino and J. Goree, Phys. Today **57**(7), 32 (2004).

7. P. Bandyopadhyay, G. Prasad, A. Sen, and P. K. Kaw, Phys. Rev. Lett. **101**, 065006 (2008).
8. J. Heinrich, S. H. Kim, and R. Merlino, Phys. Rev. Lett. **103**, 115002 (2009).
9. R. K. Varma, P. K. Shukla, and V. Krishan, Phys. Rev. E **47**, 3612 (1993).
10. F. Melandsø, Phys. Plasmas **3**, 3890 (1996).
11. P. K. Kaw and A. Sen, Phys. Plasmas **5**, 3552 (1998).
12. A. A. Mamun, R. A. Cairns, and P. K. Shukla, Phys. Plasmas **3**, 702 (1996).
13. A. A. Mamun, Astrophys. Space Sci. **268**, 443 (1999).
14. P. K. Shukla and A. A. Mamun, IEEE Trans. Plasma Sci. **29**, 221 (2001).
15. A. A. Mamun and P. K. Shukla, Phys. Lett. A. **290**, 173 (2001).
16. P. K. Shukla and A. A. Mamun, New J. Phys. **5**, 17 (2003).
17. B. Eliasson and P. K. Shukla, Phys. Rev. E **69**, 067401 (2004).
18. A. A. Mamun, B. Eliason, and P. K. Shukla, Phys. Lett A **332**, 412 (2004).
19. F. Verheest and S. R. Pillay, Phys. Plasmas **15**, 013703 (2008).
20. A. A. Mamun and R. A. Cairns, Phys. Rev. E **79**, 055401(R) (2009).
21. J. X. Ma and J. Liu, Phys. Plasmas **4**, 253 (1997).
22. S. K. El-Labany, W. F. El-Taibany, A. A. Mamun, and W. M. Moslem, Phys. Plasmas **11**, 926 (2004).
23. W. M. Moslem, Chaos, Solitons & Fractals **23**, 939 (2005).
24. A. A. Mamun and P. K. Shukla, Europhys. Lett. **87**, 2500 (2009).
25. A. A. Mamun and P. K. Shukla, New J. Phys. **11**, 103022 (2009).
26. K. S. Ashrafi, A. A. Mamun, and P. K. Shukla, Europhys. Lett. **92**, 15004 (2010).
27. H. Alinejad and A. A. Mamun, Phys. Plasmas **17**,123706 (2010).
28. M. Tribeche and A. Merriche, Phys. Plasmas **18**, 034502 (2011).
29. M. Rosenberg and D. A. Mendis, IEEE Trans. Plasma Sci. **23**, 177 (1995).
30. V. E. Fortov et al., J. Exp. Theor. Phys. **87**, 1087 (1998).
31. M. Rosenberg, D. A. Mendis, and D. P. Sheehan, IEEE Trans. Plasma Sci. **27**, 239 (1999).
32. V. W. Chow, D. A. Mendis, and M. Rosenberg, J. Geophys. Res. **98**, 19065 (1993).
33. O. Havnes et al., J. Geophys. Res. **101**, 10839 (1996).
34. T. A. Ellis and J. S. Neff, Icarus **91**, 280 (1991).
35. M. Horányi, Annu. Rev. Astron. Astrophys. **34**, 383 (1996).
36. M. Horányi, G. E. Morfill, and E. Grün, Nature **363**, 144 (1993).
37. P. K. Shukla and M. Rosenberg, Phys. Scripta **73**, 196 (2006).
38. D. J. Lacks and A. Levandovsky, J. Electrostatics **65**, 107 (2007).
39. W. M. Farrell, P. H. Smith, G. T. Delory et al., J. Geophys. Res. **109**, E03004 (2004).
40. J. Merrison, J. Jensen, K. Kinch et al., Planet. Space Sci. **52**, 279 (2004).
41. C. D. Stow, Rep. Prog. Phys. **32**, 1 (1969).
42. H. Zhao, G. S. P. Castle, and I. I. Lnculet, J. Electrostatics **55**, 261 (2002).
43. H. Zhao, G. S. P. Castle, I. I. Lnculet, and A. G. Bailey, IEEE Trans. Ind. Appl. **39**, 612 (2003).
44. S. Trigwell, N. Grable, C. U. Yurreri et al., IEEE Trans. Ind. Appl. **39**, 79 (2003).
45. F. S. Ali, M. A. Ali, R. A. Ali, and I. I. Lncullet, J. Electrostatics **45**, 139 (1998).
46. D. A. Mendis and M. Rosenberg, Annu. Rev. Astron. Astrophys. **32**, 419 (1994).
47. P. H. Sakanaka and P. K. Shukla, Phys. Scripta T **84**, 181 (2000).
48. N. D'Angelo, Planet. Space Sci. **49**, 1251 (2001).
49. A. A. Mamun and P. K. Shukla, Geophys. Res. Lett. **29**, 1870 (2002).
50. A. A. Mamun, Phys. Rev. E **77**, 026406 (2008).
51. A. A. Mamun, Phys. Lett. A **372**, 686 (2008).
52. F. Verheest, Phys. Plasmas **16**, 013704 (2009).
53. H. Washimi and T. Taniuti, Phys. Rev. Lett. **17**, 996 (1966).
54. S. Maxon and J. Viecelli, Phys. Rev. Lett. **32**, 4 (1974).
55. V. I. Karpman, *Nonlinear Waves in Dispersive Media* (Oxford: Pergamon, 1975).
56. R. Bharuthram and P. K. Shukla, Planet. Space. Sci. **40**, 465 (1992).